Nanocluster Nucleation and Growth in Polymeric Media Below the Glass Transition

Oz Gazit,[†] Nily Dan,*[,‡] and Rina Tannenbaum*[,†,§]

Department of Chemical Engineering, Technion−Israel Institute of Technology, Haifa, Israel, Department of Chemical and Biological Engineering, Drexel University, Philadelphia, Pennsylvania, and School of Materials Science and Engineering, Georgia Institute of Technology, Atlanta, Georgia

Received August 10, 2007; Revised Manuscript Received December 13, 2007

ABSTRACT: The synthesis of metal nanoclusters in a polymeric environment has been shown to yield nearly monodisperse particles, whose size is controlled by the strength of the polymer/metal interactions. Although the phenomenon is quite general, little is known regarding the mechanism by which the polymer controls nanocluster size. Previous studies of the kinetics of nanocluster growth in polymeric melts above the glass transition temperature (T_g) suggest that the nanoparticle size is set by the critical cluster size (nucleation stage) rather than the rate of metal precursor transport, namely, growth. In this paper, we examine the kinetics of iron oxide (Fe_2O_3) nanocluster formation below the glass temperature (T_g) in two polymer melts: polystyrene (PS) and poly(methyl methacrylate) (PMMA). We find that the morphology of the nanoclusters formed below T_g is highly sensitive to the system temperature and differs significantly from the morphology above T_g. However, the kinetics of cluster formation is exponential with time in both PS and PMMA, both above and below T_g. The glass transition does not significantly affect the rate constant in PS, thereby suggesting that the cluster formation mechanism is largely insensitive to the polymer state (glassy or melt). However, we find a significant difference in in the kinetics of PMMA above (where the rate constant increases exponentially with T) and below (where it is nearly constant) the T_g.

1. Introduction

In recent years, it has become increasingly evident that the use of nanoscale building blocks offers unique opportunities to engineer novel materials whose properties can be tuned through control of the structure at intermediate length scales that bridge between the molecular and the bulk.[1,2] This is due to the fact that the characteristic properties of nanoscale clusters are significantly affected by their size, shape, and spatial dispersion.[3−7] For example, Cox et al.[6] found that clusters of 12−32 atoms of rhodium exhibit magnetic moments that are typical of ferromagnetic materials, although bulk rhodium is paramagnetic at all temperatures. As a result, material properties can be set by the size of the underlying nanodomains.

One class of nanostructured materials that holds great promise for a variety of applications is that of metallic/polymeric nanocomposites, where nanoscale metallic clusters are dispersed in a polymeric medium.[8−10] The synthesis of such polymer−metal nanocomposites can be accomplished by several methods: (a) evaporation of metal atoms into polymer solutions[11−16] or on polymeric films,[17] (b) addition of polymers to solutions of metal salts followed by the reduction of the salts to colloidal nanoparticles and evaporation of the solvent,[18] (c) synthesis of metal clusters within an SiO_2 matrix by sol−gel processes,[19] (d) reduction and aggregation of the metal complexes in the solid state within an organometallic polymer matrix,[3,4] and (e) in situ thermolysis of organometallic precursors in a polymeric melt/solution.[5]

Due to the strong dependence of the metallic cluster properties on cluster size, obtaining polymeric nanocomposites with specific material properties requires the ability to control the *size and polydispersity* of the nanoclusters. Unfortunately, classical nucleation and growth processes usually yield clusters with a wide size distribution and diverse morphologies,[7] thereby limiting the use of the nanocomposites for applications such as photonic materials.[5,7]

In situ synthesis of metal nanosclusters in polymeric media (either bulk melt or solution) has been shown to produce clusters with a narrow size distribution and uniform morphology in a wide range of polymer and metal systems.[5,20−23] Although cluster size was found to depend on such parameters as polymer type, polymer concentration and MW, and the temperature of the in situ synthesis,[5,21] the narrow size distribution was shown to be independent of metal volume fraction and synthesis conditions.[5,24] Thus, in situ synthesis of metal nanoclusters in polymeric media offers a route for obtaining uniform, controllable nanocomposites. However, tailoring nanocomposite properties requires better understanding of the nanocluster synthesis process and, specifically, the parameters controlling the cluster size and size distribution.

Previous studies clearly demonstrate that the average size of metallic nanoclusters synthesized in polymeric media decreases with increasing strength of polymer/metal bonds (the use of the term metal nanoclusters comprises both zero valent metal particles and metal oxide particles).[5,24] This may be simply attributed to the propensity of such systems to increase the interfacial area between the clusters and the favorable polymeric media, but it cannot explain the apparent cluster monodispersity. The universality of the narrow nanocluster size distribution when synthesized in *any* polymeric medium (solution or bulk) suggests that the mechanism controlling cluster size is not polymer specific. Rather, it arises from the macromolecular nature of the medium.

"Polymeric capping" has been suggested as a possible mechanism for the control of cluster growth, where polymer adsorption on the metal or metal oxide surface hinders transport of precursor atoms and thus limits growth beyond a specific

* To whom correspondence should be addressed. E-mail: rinatan@technion.gatech.edu; dan@coe.drexel.edu.
[†] Technion−Israel Institute of Technology.
[‡] Drexel University.
[§] Georgia Institute of Technology.

10.1021/ma071816o CCC: $40.75
Published on Web 02/22/2008

size set by the polymer−metal interactions.[21] However, while this mechanism can explain the absence of particles that are larger than the optimal size set by the "cap," it cannot address the lack of *smaller* particles in finite systems where the volume fraction of metal is fixed.[21]

Most studies of metal or metal oxide cluster synthesis in polymeric media tend to focus on equilibrium properties (i.e., cluster size and morphology)[24,25] and thus offer little insight into the process of cluster formation. On the other hand, kinetic studies can reveal essential information on the mechanism of cluster nucleation and growth. We have previously reported on the decomposition kinetics of iron pentacarbonyl to iron oxide nanoclusters (γ-Fe_2O_3) above the glass transition temperature (T_g) in two types of polymeric melts: polystyrene (PS) and poly(methyl methacrylate) (PMMA).[24] In all temperatures studied, clusters synthesized in PS were found to be roughly spherical while those synthesized in PMMA were more triangular in shape. Since PS interacts weakly with the iron oxide cluster, the particles formed were larger, on the order of 70 nm. Particles formed in PMMA, which interacts strongly with the metal, were found to be smaller, on the order of 11 nm.[24]

Following the time-dependent precursor concentration (which is negatively proportional to the fraction of metal in clusters) showed an exponential decay with time for all temperatures studied.[24] Analysis using a simple nucleation and growth model suggests that this type of kinetics is the signature of a system dominated by the nucleation stage, where growth is largely suppressed.[24] The characteristic decay time scale was found to be higher (slower reaction) in PMMA than in PS and was found to decrease, in both polymers, with increasing decomposition temperature. The decay time was found to vary as $\sim e^{A/T}$, where $A \approx 9000$ °K for PS and 8100 °K for PMMA.

The mobility of molecular species in polymeric media decreases sharply below T_g, the glass transition temperature.[26−30] Thus, the synthesis of metallic nanoclusters in polymeric media below T_g should be dominated by nucleation rather than growth. If, indeed, nucleation dominates cluster formation below T_g (as it does above T_g[24]), then the kinetic signatures of the decomposition process should be insensitive to whether the system is above or below T_g (although the time constants would still vary with the temperature, as shown for the systems above T_g[24]).

In this work, we examine the decomposition kinetics and particle morphology of iron oxide (γ-Fe_2O_3) nanocluster formation in PS and PMMA below the polymer glass transition (T_g). The reduction in polymer mobility may affect the cluster properties and the synthesis kinetics in several ways. First, regardless of the cluster growth mechanism, the suppressed polymer mobility should hinder the growth of the cluster (since the polymer cannot "move out of the way" of the growing cluster). As a result, we expect clusters formed below T_g to be smaller than those formed above T_g. Also, the clusters may be more anisotropic, since growth is likely to follow structural heterogeneities (e.g., craze lines) of the polymer matrix. Also, below T_g, the polymer cannot adjust to form an adsorbed "cap" on the growing cluster.[31−33] Thus, if capping is indeed a dominant mechanism, it should be suppressed below T_g, leading to a higher cluster polydispersity and to a reduced sensitivity of the cluster size to the polymer−metal interactions.

2. Experimental Methods

2.1. Preparation of Composite Films. Pellets of poly(methyl methacrylate) ($\bar{M}_n = 350\,000$ g/mol, $d = 1.170$ g/cm^3, Aldrich) or polystyrene ($M_n = 350\,000$ g/mol, $d = 1.047$ g/cm^3, Aldrich) were initially dissolved in methylene chloride (CH_2Cl_2, $d = 1.325$ g/cm^3, bp = 40 °C, Aldrich, 99.6%) to form 3 wt % polymer solutions. Iron pentacarbonyl ($Fe(CO)_5$, $d = 1.45$ g/cm^3, bp = 103 °C, Alfa Products, Thiokol/Ventron Division) was filtered through filter paper circles (Whatman 7.0 cm, qualitative 4) into a foil-covered 8 mL vial. One mL of the filtered $Fe(CO)_5$ was then added dropwise into the polymer solution. After mixing vigorously for approximately 30 min, the $Fe(CO)_5$/polymer solution was film cast onto a glass surface and the solvent was allowed to evaporate under inert conditions. Film thickness average was 0.100−0.150 ±0.002 mm.

Thermal decomposition was carried out in a temperature-controlled oven under an ambient (oxidative) room atmosphere. Films were covered with aluminum foil to prevent photodecomposition. $Fe(CO)_5$ has a relatively high vapor pressure at room temperature, so some of the original carbonyl was lost due to evaporation prior to decomposition. Thermal treatment was done below the polymer T_g at temperatures ranging from 50 to 95 °C. The kinetic behavior was analyzed based on the actual $Fe(CO)_5$ concentration, as measured by the intensity of its analytically relevant infrared absorption bands. The rate of $Fe(CO)_5$ precursor decomposition was determined by monitoring the variations in the intensity of the two strong infrared absorption bands at 2019 and 1996 cm^{-1}, corresponding to the asymmetric and symmetric stretching vibrations of the carbonyl groups, respectively. Infrared measurements were conducted on a Nicolet Nexus 870 Fourier transform infrared spectrophotometer. Further details regarding the decomposition reaction may be found in the pertinent references.[34,35]

2.2. Particle Characterization. Particle size and morphology were examined by transmission electron microscopy (TEM) using both Philips CM-120 and FEI Tecnai G^{2}T12 instruments. The operating voltage was 120 kV for both microscopes. Samples were ultramicrotomed to a thickness of 50−70 nm using a Reichert−Jung FC4E knife under a constant temperature of −80 °C and subsequently placed on 400-mesh carbon-coated copper grids (Ted Pella, Inc).

2.3. Polymer Thermal Properties. The glass transition temperature (T_g) of the composite films was determined by differential scanning calorimetry (DSC) using a Mettler Toledo DSC822e instrument for the PS films and Perkin-Elmer DSC 7 instrument for the PMMA film with air as the reference. The measurements were performed upon heating from 60 to 210 °C and then cooling back to 60 °C. Heating rate was set to 5 °C/min for the PS and 20 °C/min for the PMMA. The heating/cooling cycle was repeated twice to allow the sample to arrange itself in the crucible, which ensured a better heat conductance during the actual test. Nitrogen was used as the purge gas at 40 mL/min. Ideally, T_g is measured during the cooling period,[36] but in this case the films were analyzed both during cooling and heating, and both directions showed no significant difference.

3. Results and Discussion

The goal of this paper was to examine the synthesis of iron oxide nanoclusters in polymeric media below the glass transition temperature. However, it is well known that the presence of small molecule "impurities," even in very low concentrations, can reduce the T_g of the polymer matrices in which they are embedded.[37,38] The main concern here was that a decrease in the glass transition temperature of the precursor-containing polymer samples below the decomposition temperatures would have resulted in a kinetic behavior that was not representative of the glassy state. Since the resulting composites were investigated also for their optical properties, it was desirable to examine relatively thin films rather than bulk material. Hence, the thickness of our films ($\sim 100\ \mu$m) was in the range at which the glass transition may deviate from the bulk value and depend on the film thickness.[39] Therefore, to ensure that the temperature range at which we conducted the decomposition process was indeed below the glass transition of the polymer system, we first examined the glass transitions of our composite films using DSC. The thermolysis process of the organometallic precursors

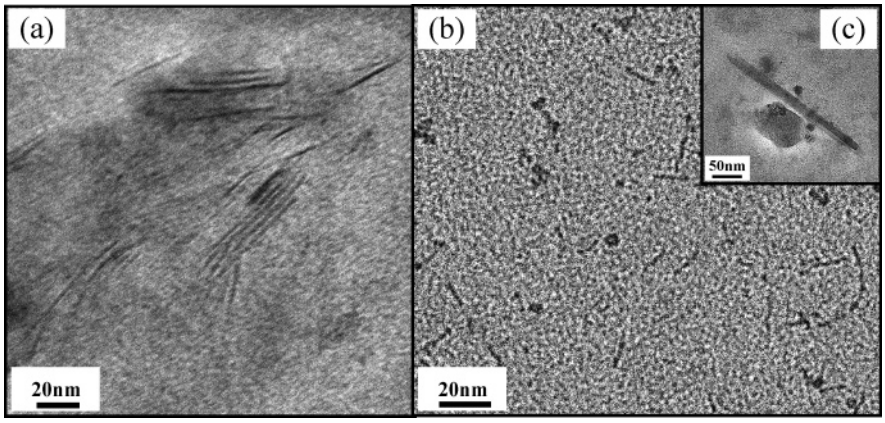

Figure 1. Transmission electron micrographs (TEM) of iron oxide particles formed after the decomposition of $Fe(CO)_5$ in a PS matrix at two extreme temperatures below the glass transition of the polymers: (a) iron oxide nanoparticles formed in PS at 50 °C, (b) iron oxide nanoparticles formed in PS at 95 °C, and (c) detailed image of iron oxide nanoparticles formed in PS at 95 °C.

dispersed in the polymer matrix involves the formation of reactive metallic fragments capable of interaction with the polymer, resulting in the formation of local physical cross-links between chains that, in turn, could generate an increase in the material T_g.[40] However, given the concurrent presence of the two effects, the possible plasticizing effect of the small precursor molecules may have been offset by the possible local increase in T_g due to the crosslinking effect of the reactive fragments, leaving the T_g of the samples unchanged. Since during the DSC measurements we did not record any melting or crystallization temperatures or any shifts in the T_g of the polymer, we concluded that the low concentration of metallic particles (~5 vol %) and the thickness of our films have little effect on the T_g of the samples. As shown in Table 1, we found that the glass transition temperatures of PS and PMMA films containing the organometallic precursors were relatively close to that of polymer films in the absence of these precursor molecules.[39] All of our decomposition and cluster synthesis experiments, discussed below, were carried out at temperatures below the measured T_g of the polymer matrices. Furthermore, examination of films after thermal treatment showed that T_g was still above the temperature at which the experiment was conducted.

We first examined the properties of the (final) iron oxide clusters, namely, their morphology and dimensions at the end of the decomposition process. In our previous work, the synthesis of iron oxide nanoparticles in PS melts at temperatures above T_g has been shown to yield roughly spherical clusters, with a characteristic diameter of ~70 nm.[24,41] In contrast, clusters formed in PMMA at temperatures above T_g were roughly triangular in shape, with an average size of 11 nm. The difference in cluster dimensions and geometry was attributed chiefly to the strength of the polymer/cluster interfacial binding γ, which is higher for PMMA.[24,41]

Figure 1 shows transmission electron micrographs (TEM) of clusters formed in the PS matrix below T_g. We found that in the lower temperature range, i.e., 50 °C, the clusters were needlelike with an average length of ~50 nm and a cross-sectional width of 2−3 nm (Figure 1a). Increasing the temperature to the higher range, i.e., 95 °C (below the T_g, as shown in Table 1) leads to the appearance of spherical clusters, with an average diameter of ~8 nm, that coexist with a decreased fraction of the small needlelike clusters (Figure 1b). We also observe some larger triangular aggregates, as shown in Figure 1c.

Particles formed in the PMMA matrix below T_g follow a similar trend to that of those formed in PS. In the lower temperature range, i.e., 50 °C, the iron oxide nanoparticles aggregate in small chains that are ~ 40 nm in length and ~3 nm in width (panels a and c of Figure 2). At higher temperatures, the chains disappear and only small spherical particles with ~5 nm average diameter are observed, some of which assembled in larger flocculates (panels b and d of Figure 2).

Table 1. Onset Value for the Glass Transition Temperatures of PMMA and PS Thin Films before and after Thermal Treatment in the Presence of Iron Carbonyl Precursor Determined by Differential Scanning Calorimetry

decomposition temperature (°C)	T_g of PMMA film (°C)	T_g of PS film (°C)
literature[39]	115	100
50	110.40	97.11
67	117.99	99.07
82	116.08	97.72
95	119.88	97.19

Our microscopy results suggest that at low temperatures where the polymer is immobilized in the glassy state[42,43] clusters are largely one-dimensional. Most likely, cluster morphology follows defects such as structural inhomogeneities or "craze lines" in the glassy polymer matrix (generated by internal stresses), a mechanism that is illustrated in Figure 3.[31−33,44−46] While at temperatures above T_g the equilibrium particle size is determined by the interactions between the metallic fragments and the polymer chains (Figure 3a,b), below T_g the immobilized polymeric medium acts as a heterogeneous surface that promotes the formation of many reactive nucleation centers and as a physical "capping" medium defined by the geometry of the system (Figure 3c,d).[44−46]

This may also explain the large polydispersity in cluster dimensions and morphology, since the cluster geometry is not set by nucleation and growth but by the properties of the polymeric matrix defects. Increasing the system temperature increases polymer mobility, especially in the vicinity of the cluster crossing point,[47−49]which enables the formation of three-dimensional clusters. However, the polymer-imposed constraints on cluster size are evident even when T approaches T_g by the smaller size of the clusters compared to those formed above T_g. Moreover, since reactions between the functional groups of the polymer and the growing metallic fragments are suppressed at low temperatures,[47,48] the stabilization of the nanoparticles is due mainly to the geometric confinement imposed by the polymer 'wall' and not because of the adsorption of polymer chains.

Our TEM data clearly demonstrates that the size and morphology of metallic clusters formed in polymeric matrices

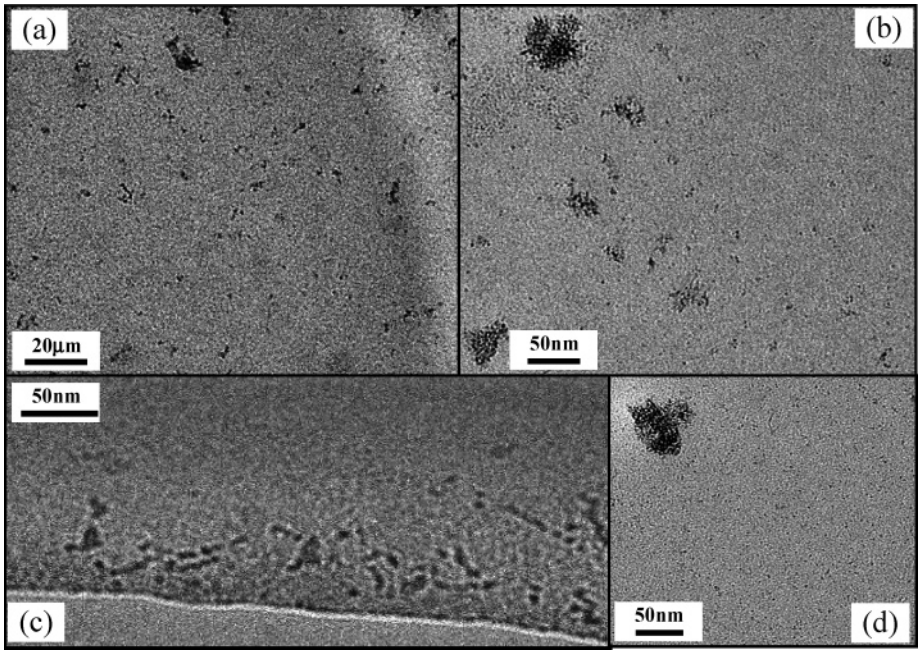

Figure 2. Transmission electron micrographs (TEM) of iron oxide particles formed after the decomposition of $Fe(CO)_5$ in a PMMA matrix at two extreme temperatures below the glass transition of the polymers: (a) iron oxide nanoparticles formed in PMMA at 50 °C, (b) iron oxide nanoparticles formed in PMMA at 95 °C, (c) detailed image of iron oxide nanoparticles formed in PMMA at 50 °C, and (d) detailed image of iron oxide nanoparticles formed in PMMA at 95 °C.

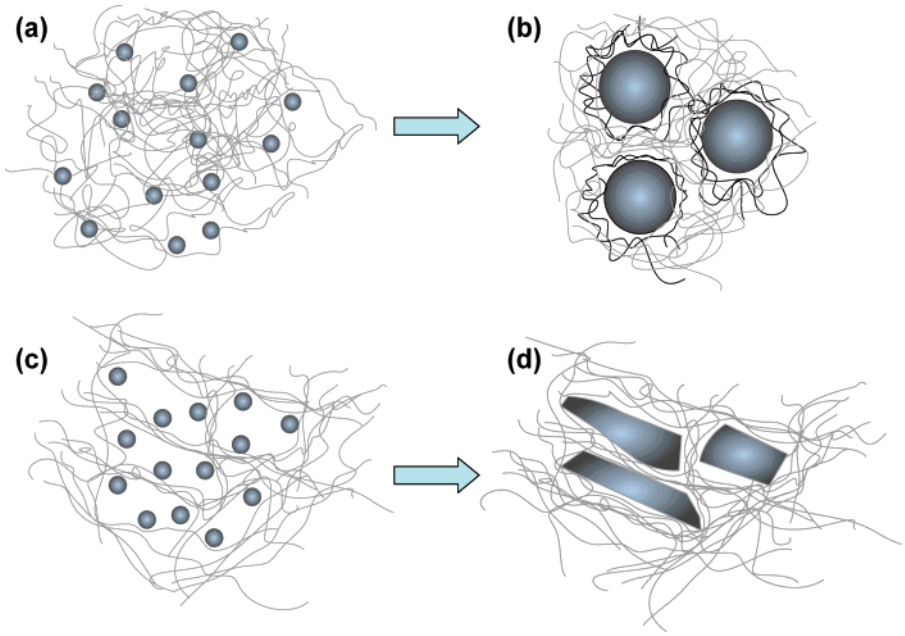

Figure 3. The differences in the nucleation and growth mechanisms between temperatures. Above T_g: (a) highly reactive metallic nucleation centers are formed; (b) particle−polymer interactions determines equilibrium particle size. Below T_g: (c) the immobilized polymeric medium that acts as a heterogeneous surface and promotes the formation of many highly reactive nucleation centers; (d) Physical "capping" defined by grain boundaries determined by the polymer arrangement .

below T_g differ from those of the clusters formed in the same matrices above T_g. To determine whether these differences are due to the geometrical confinement of clusters by the glassy polymer or are the result of a difference in the synthesis mechanism, requires a study of the kinetics of cluster formation.

The formation of iron oxide clusters starts with the extraction of at least one CO ligand from the inorganic precursor $Fe(CO)_5$ followed by a series of ligand dissociation and complex rearrangements, giving rise to coordinatively unsaturated, multinuclear iron complexes having a higher metal/ligand ratio than the original precursor.[20,22,50] These iron fragments are highly reactive,[11] generating a nucleation and growth process. In systems such as ours, the ambient oxidizing environment gives rise to the oxidation of the active Fe fragments to form nanoclusters consisting mainly of Fe_2O_3. This can be summarized as follows:

$$n\mathrm{Fe(CO)_5} \underset{k_{-1}}{\overset{T,\,k_1}{\rightleftharpoons}} n\mathrm{Fe(CO)_{m\le 4}} \xrightarrow[k_{-2}]{k_2} \left(\frac{n}{x}\right) \mathrm{Fe_x(CO)_y} \xrightarrow{O_2,\,k_3} \left(\frac{n}{2z}\right)(\mathrm{Fe_2O_3})_z$$

Fe "precursor" — Coordinatively unsaturated species — Fe "active" fragments or "metallomers"

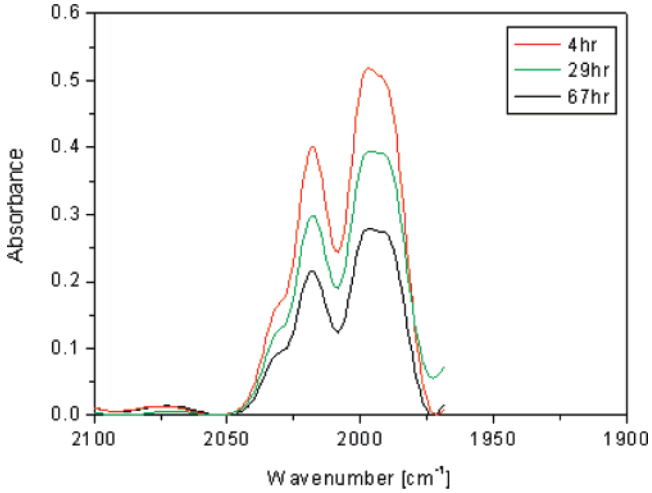

Figure 4. Typical infrared absorption spectra of the thermal decomposition of $Fe(CO)_5$ in polystyrene at 82 °C showing the symmetric and asymmetric stretching bands of $Fe(CO)_5$ at 1996 and 2019 cm^{-1}, respectively.

The kinetics of cluster formation are determined by following the symmetric and asymmetric CO stretching bands of $Fe(CO)_5$ at 1996 and 2019 cm^{-1}, respectively, the CO stretching bands of $Fe_3(CO)_{12}$ (the most dominant intermediate) at 2046 cm^{-1}, and Fe−O stretch of iron oxide at 520 cm^{-1}.[51−53] Monitoring can also be done by following the stretching and bending of the Fe−CO equatorial ligands using the 641 cm^{-1} absorption band,[54−57] but this one has a weak absorbance and gives the exact same result.

As shown in Figure 4, the $Fe(CO)_5$ infrared absorbance peak clearly decays, as expected, with decomposition time. We do not observe a peak associated with decomposition intermediates, thereby suggesting that these do not accumulate in the system. Unfortunately, the iron oxide characteristic absorption band cannot be used to analytically determine cluster growth since it resides at the lower mid-IR region, near the end of our instrument range, and thus is exposed to beam cutoff.[58] However, due to the lack of intermediates, mass balance on the iron atoms indicates that the number of iron atoms in the clusters is equal to the initial iron content minus the remaining $Fe(CO)_5$,[24] and thus $\partial\phi_{cluster}/\partial t \approx -\partial\phi_{percursor}/\partial t$, where ϕ is the concentration of the species and t the time.[24]

Figure 5 shows the plots of the normalized concentrations of $Fe(CO)_5$ in both PS (Figure 5a) and PMMA (Figure 5b) matrices as a function of time for several temperatures below T_g. We see that in both polymers the decay of the precursor (and thus the rate of cluster formation) follows an exponentially decaying function. This trend is similar to that observed for the same systems above T_g.[24] Above T_g, the rate of decomposition (and thus cluster formation) in PS was found to be higher than that in PMMA at the same decomposition temperature due to the weaker interfacial interactions of PS with the metal cluster.[24] Below T_g, we expected the polymer chains to be largely immobilized, thereby reducing the effect of the interface on the decomposition and cluster formation rates. However, as shown in Figure 5c, the precursor decomposition below T_g in PS was still faster than in PMMA, again at the same decomposition temperature.

Fitting the $Fe(CO)_5$ decay to an exponential function $f_{precursor}(t) = \phi_0 e^{-kt}$ yields values of the kinetic rate constant k as a function of the system temperature. Here, k represents the rate constant of the $Fe(CO)_5$ decomposition, which may be expected to be exponential.[24,25] However, since there is no accumulation of

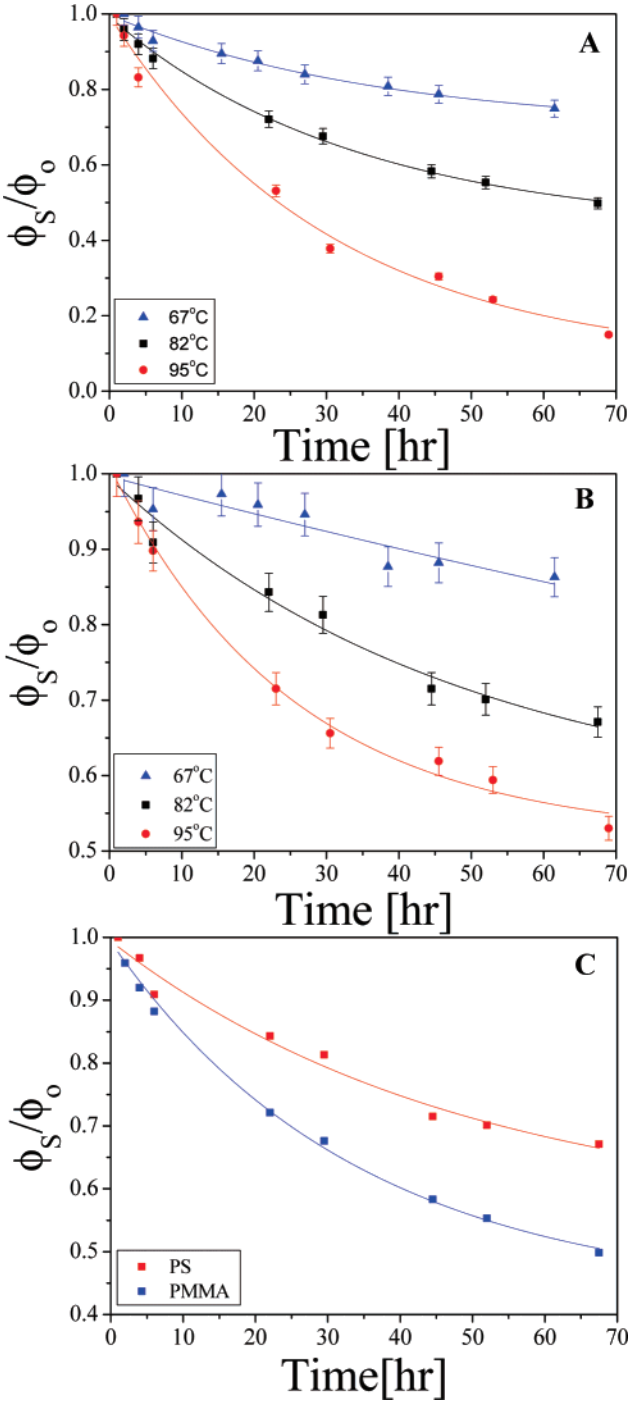

Figure 5. Plots of the normalized concentrations of $Fe(CO)_5$ in polymer matrices as a function of decomposition time at different temperatures below the glass transition temperature of the respective polymers: (a) in a PS matrix, (b) in a PMMA matrix, and (c) comparison between the decomposition of $Fe(CO)_5$ in the PS matrix and in the PMMA matrix at 82 °C.

intermediates in the system, k also represents the time constant of cluster synthesis, a result of both nucleation and growth processes. Thus, the fact that the precursor decay profile is exponential both above and below T_g indicates that the mechanism of cluster synthesis is similar. We have previously shown[24] that an exponential cluster synthesis rate is characteristic of systems where nucleation, rather than growth, is dominant. As was stated in our previous work,[24] cluster growth through molecular addition is controlled by the diffusional flux of metallic fragments to the growing clusters. The full diffusion/growth problem is complex and cannot be solved analytically,

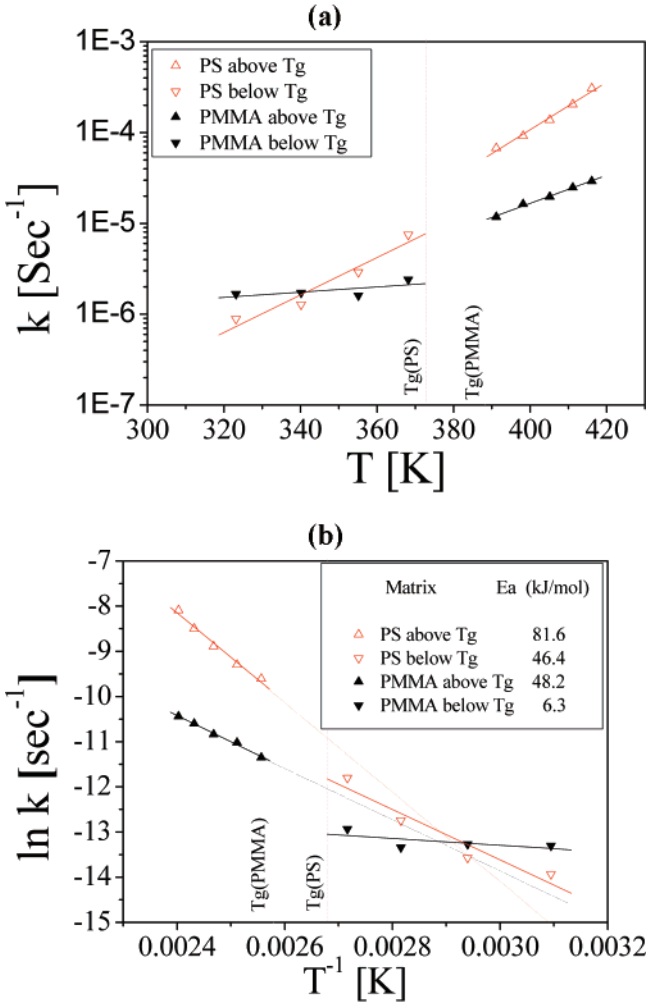

Figure 6. (a) Plot of the characteristic decay constant k (in units of s^{-1}) as a function of temperature for both polymeric matrices. (b) The Arrhenius plot for the decomposition processes showing the logarithm of the characteristic decay constant ln k (in units of s^{-1}) as a function of the inverse temperature for both polymeric matrices.

since it involves a moving boundary, namely, the cluster radius, as well as the time-dependent concentration of the diffusing fragments. However, applying a simplified approach, we can define the flux to the growing cluster through a "boundary layer," where the concentration of unstable and reactive iron fragments at the cluster interface is zero, and outside the boundary layer it is given by the average suspension concentration.[24] This kind of analysis allows the calculation of the extreme cases in the system, namely, the reaction mechanism controlled by either nucleation or growth (the interested reader may turn to the full analysis described in our previous paper[24]). This kind of analysis seems very plausible for the clusters in glassy polymers, where the transport of molecular species and thus growth is very slow.

As may be expected and as observed from Figure 6a, the rate constant k, which is inversely proportional to the characteristic decomposition time and/or cluster formation time, increases with increasing temperature. Thus, cluster formation rates increase with T in both types of polymeric media. In PS, we find little difference in the dependence of k on T above and below T_g: below T_g, $k = 7 \times 10^{-8}\ e^{0.047T}$, and above T_g, $k = 5 \times 10^{-8}\ e^{0.06T}$. The range of temperatures at which we conducted our experiments lied below T_α, typically attributed to T_g, and in some cases above the lower temperature of T_β, typically attributed to secondary and higher-order relaxations, which are assumed to involve only local molecular motions. For both PS and PMMA systems, this range of temperatures is characterized by the occurrence of micro-Brownian behavior, resulting from the fact that some of the chains are not completely immobilized in the glassy state and hence small segments therein are free to move. For amorphous polymers, such as PS and PMMA, this local motion of chains is associated with the movement of side chains around the backbone of the polymer.[40,59] The exponential behavior described previously indicates that the kinetics of iron oxide cluster formation in PS matrices is largely insensitive to the transition from temperatures above to below T_g. In the higher range of temperatures that we examined, for PS it is very close to its T_g (and most likely above T_β) and therefore, the polymer chains exhibit micro-Brownian behavior. Due to the weak interactions of PS with the metal, the physical state of the polymer, either below T_g or in the melt, has little effect on the kinetics. However, since Figure 6a clearly shows exponential dependence for the reaction in PS above and below T_g and for PMMA above T_g, we can fit the data to an Arrhenius plot, as shown in Figure 6b, and calculate the reaction activation energies, E_a. From Figure 6b, it is evident that for PS below T_g the activation energy is close to half the value as compared to that above T_g, i.e., $E_a = 46.4$ and 81.6 kJ/mol, respectively. The kinetics in the PS matrix is nevertheless largely unaffected by the physical state of the polymer, despite the occurrence of the micro-Brownain chain motion that affords the movement of a fraction of the polymer chains. However, the lower activation energy is attributed to the fact that the majority fraction of chains are in the glassy state and are not able to conform and interact with the reacting metal cluster.

In PMMA, however, we find a significant difference in the dependence of k on T across the glass transition: above T_g, $k = 2 \times 10^{-7} e^{0.035T}$, namely, the characteristic cluster formation time scale decreases exponentially with the decomposition temperature. The values of k for PMMA above T_g are lower than that for cluster formation in PS at the same temperature, indicating that the formation of clusters in PMMA is a slower process and is most likely due to the stronger interfacial bonding between the metal cluster and PMMA when compared to that in PS (as shown in Figure 5c).[24]

Quite surprisingly, however, in the PMMA system below T_g, we find that k is a *constant*, namely, the cluster formation kinetics are independent of the system temperature. One explanation may be that, since the T_g of PMMA is higher than that of PS, the PMMA systems were truly in the glassy state at the temperatures measured while the PS systems were still close to the glass transition. Following this argument, if the only important feature would have been the distance from the actual polymer T_g, then plotting k as a function of $\Delta T = T - T_g$ should have generated a "universal curve," i.e., the same trend for similar ΔT values. However, as shown in Figure 7, the plot of k as a function of ΔT reveals a considerable discrepancy between the two polymers, which cannot be accounted for by the distance of the decomposition temperature from T_g.

Our finding that k in PMMA is independent of T below the glass transition clearly indicates that the dominant mechanism, or rate-limiting step, in the cluster formation is *not* the precursor decomposition: Precursor decomposition requires overcoming some energy barrier (i.e., activation energy) to allow the iron pentacarbonyl molecule to transition into one of the reactive intermediates. This should be accelerated exponentially (Arrhenius) with increasing T regardless of the environmental mobility. Moreover, this conclusion is also supported by the calculation of the activation energy. In Figure 6b, we found for

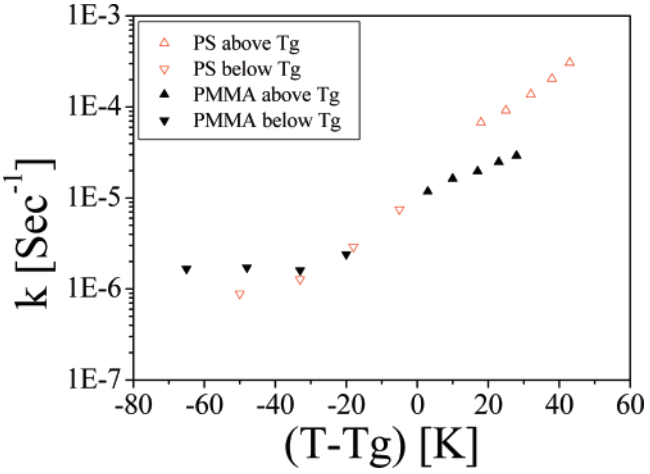

Figure 7. A universal curve describing the relationship between the decomposition reaction constant k (in units of s^{-1}) and the distance of the reaction temperature from the actual polymer T_g, i.e., $\Delta T = T - Tg$.

PMMA below T_g $E_a = 6.3$ kJ/mol, which is an order of magnitude smaller than the one found for above T_g, $E_a = 48.2$ kJ/mol. Thus, the rate-limiting step in the system is the cluster formation, which apparently occurs via a different mechanism than that taking place in PMMA above T_g or in PS at all temperatures.

As mentioned above, we have previously concluded that the exponentially decaying precursor concentration as a function of time is a signature of cluster formation that is dominated by the nucleation rather than growth step.[24] The kinetic constant was calculated to be $k \sim (\gamma/\epsilon)^3 \exp[-(\gamma^3)/(\epsilon^2 k_B T)]$,[24] where γ is the polymer/cluster interfacial tension, ϵ is the iron−iron bond energy in the cluster (actually, it is the energy of the iron−iron bonds in the "metallomers"), and k_B the Boltzmann constant. ϵ is expected to be independent of T. If γ is also independent of T, k will increase exponentially with T, as observed in PS at all temperatures and in PMMA above T_g. For PMMA below T_g, this suggests that $\gamma \sim T^{1/3}$ (thus eliminating the exponential relationship). The remaining linear dependence of k on T due to the pre-exponential constant is in agreement with the observed data. We therefore need to explain why the interfacial tension between the polymeric media and the iron oxide cluster is roughly independent of T for PS above and below T_g and for PMMA above T_g but increases with T for PMMA below the glass transition.

The interactions between PS and iron oxide clusters are dominated by dipole−dipole interactions. The relatively weak nature of these interactions allows more flexibility in regards to the geometrical fit between polymer segments and surface sites on the cluster. However, in the case of PMMA, the interactions with the clusters consist of a stronger coordination bond, which requires a tighter geometric fit between the polymer functional groups and reactive metallic sites.[60−62] Above T_g, the PMMA chains are free to rearrange on the cluster surface, so that γ is a constant. However, below T_g, the mobility of the chains is constrained, thereby reducing the value of γ (as shown in Figure 3). With increasing temperature, entering into the micro-Brownian regime, the mobility of the PMMA chains at the cluster interface increases, thereby leading to a better fit and an increase in the value of γ. Since the temperatures we used are farther from T_g for PMMA than for PS, it is reasonable that more of the PMMA chains are in the glassy state than the PS chains at the same temperature. This explains the dramatic change occurring in the activation energy (Figure 6b) calculated for the PMMA system for the temperatures below T_g to that calculated for the temperatures above T_g, which is in contrast to the change calculated for PS.[59,63]

4. Conclusions

In this paper, we examined the kinetics of metal-cluster formation in polymeric matrices below the glass transition temperature. We showed that the morphology of the nanoclusters formed under these conditions is dependent on the decomposition temperature and differs significantly from their morphology above T_g, which is most likely due to cluster formation at the interface between regions of inhomogeneities, craze lines, and stress-induced ordered regions. However, the kinetics of cluster formation is exponential with time for both PS and PMMA above and below T_g. The glass transition does not significantly affect the rate constant k in PS, thereby suggesting that the cluster formation mechanism is largely insensitive to the polymer state (glassy or melt). However, we find a significant difference in the dependence of k in PMMA above T_g (where it increases exponentially with T) and below T_g (where it is nearly constant). We attribute this to the effect of the polymer glassy state on the polymer−cluster interfacial forces, which are weakened by the suppressed mobility of the PMMA segments in the glassy state.

Acknowledgment. The authors appreciate the initial interest that David Droz expressed in this research during his stay at the Technion. The authors are grateful to the Louis and Bessie Stein Foundation for their generous financial support to David Droz and Nily Dan of Drexel University. This research was also supported by the Israel Science Foundation, Grant No. 650/06, by a European Union Marie Curie International Reintegration Grant (IRG) No. 036577, and the National Science Foundation, Award No. ECS-0535382.

References and Notes

(1) Joannopoulos, J. D.; Meade, R. D.; Winn, J. N. *Photonic Crystals-Molding the Flow of Light*; Princeton University Press: Princeton, N.J., 1995; p 3.
(2) Misner, M. J.; Skaff, H.; Emrick, T.; Russel, T. P. *Adv. Mater.* **2003**, *15* (3), 221.
(3) Cheong Chan, Y. Ng.; Craig, G. S. W.; Schrock, R. R.; Cohen, R. E. *Chem. Mater.* **1992**, *4*, 885.
(4) Liu, K.; Clendenning, S. B.; Friebe, L.; Chan, W. Y.; Zhu, X.; Freeman, M. R.; Yang, G. C.; Yip, C. M.; Grozea, D.; Lu, Z.-H.; Manners, I. *Chem. Mater.* **2006**, *18*, 2591.
(5) Tannenbaum, R.; Zubris, M.; Goldberg, E. P.; Reich, S; Dan, N. *Macromolecules* **2005**, *38*, 4254.
(6) Cox, A. J.; Louderback, J. G.; Apsel, S. E.; Bloomfield, L. A. *Phys. Rev. B* **1994**, *49*, 12295.
(7) Service, R. F. *Science* **1996**, *271*, 920.
(8) Garcia-Moreno, I.; Costela, A.; Cuesta, A.; Garcia, O.; del Agua, D.; Sastre, R. *J. Phys. Chem. B* **2005**, *109*, 21618.
(9) Gómez-Romero, P.; Cuentas-Gallegos, K.; Lira-Cantú, M.; Casañ-Pastor, N. *J. Mater. Sci.* **2005**, *40*, 1423.
(10) Zhang, J.; Coombs, N.; Kumacheva, E. *J. Amer. Chem. Soc.* **2002**, *124*, 14512.
(11) Klabunde, K. J.; Habdas, J.; Cardenas-Trivino, G. *Chem. Mater.* **1989**, *1*, 481.
(12) Andres, M. P.; Ozin, G. A. *Chem. Mater.* **1989**, *1*, 174.
(13) Bradley, J. S.; Hill, E.; Leonowicz, M. E.; Witzke, H. *J. Mol. Catal.* **1987**, *41*, 59.
(14) Hable, C. T.; Wrighton, M. S. *Langmuir* **1991**, *7*, 1305.
(15) Noguchi, T.; Gotoh, K.; Yamaguchi, Y.; Deki, S. *J. Mater. Sci. Lett.* **1991**, *10*, 447.
(16) Perrin, J.; Despax, B.; Kay, E. *Phys. Rev. B* **1985**, *32*, 719.
(17) Horiuchi, S.; Sarwar, M. I.; Nakao, Y. *Adv. Mater.* **2000**, *12* (20), 1507.
(18) Van Rheenen, P.; McKelvy, M.; Marzke, R.; Glaunsinger, W. S. *Inorg. Synth.* **1986**, 238.
(19) Tour, J. M.; Pendalwar, L. S.; Copper, J. P. *Chem. Mater.* **1990**, *2*, 647.

(20) Tadd, E. H.; Zeno, A.; Zubris, M.; Dan, N.; Tannenbaum, R. *Macromolecules* **2003**, *36*, 6497.
(21) Gubin, S. P. *Colloids Surf., A* **2002**, *202*, 155.
(22) Heck, R. F.; Breslow, D. S. *J. Amer. Chem. Soc.* **1961**, *83*, 4023.
(23) Klaubunde, K. J.; Tanaka, Y. *J. Mol. Catal.* **1983**, *21*, 57.
(24) Dan, N.; Zubris, M.; Tannenbaum, R. *Macromolecules* **2005**, *38*, 9243.
(25) Tannebaum, R.; Hakanson, C.; Zeno, A.; Tirrell, M. *Langmuir* **2002**, *18*, 5592.
(26) Young, R. J.; Lovell, P. A. *Introduction to Polymers*, 2nd ed.; Chapman and Hall: New York, 1991; p 292; Hiemenz, P. C. *Polymer Chemistry*; Marcel Dekker: New York, 1984; p 244.
(27) Kerle, T.; Lin, Z.; Kim, H.-C.; Russell, T. P. *Macromolecules* **2001**, *34* (10), 3484.
(28) Tsui, O. K. C.; Wang, X. P.; Ho, J. Y. L.; Ng, T. K.; Xiao, X. *Macromolecules* **2000**, *33* (11), 4198.
(29) Schlotter, N. E.; Furlan, P. Y. *Polymer* **1992**, *33* (16), 3323.
(30) George, S. C.; Thomas, S. *Prog. Polym. Sci.* **2001**, *26* (6), 985.
(31) Kambour, R. P.; Holik, A. S. *J. Polym. Sci., Part B: Polym. Phys.* **1969**, *7* (8), 1393−403.
(32) Di Filippo, G. V.; Vander Sande, J. B.; Uhlmann, D. R. *J. Appl. Polym. Sci.* **1988**, *35* (2), 485−505.
(33) Renninger, A. L.; Uhlmann, D. R. *J. Polym. Sci., Part B: Polym. Phys.* **1978**, *16*, 2237−2244.
(34) Tannenbaum, R.; Flenniken, C. L.; Goldberg, E. P. *J. Polym. Sci., Part B: Polym. Phys.* **1990**, *28*, 2421.
(35) King, S.; Hyunh, K.; Tannenbaum, R. *J. Phys. Chem. B* **2003**, *107*, 12097.
(36) Montserrat, S.; Calventus, Y.; Hutchinson, J. M. *Polymer* **2005**, *46*, 12181.
(37) Sangermano, M.; Malucelli, G.; Amerio, E.; Priola, A.; Billi, E.; Rizza, G. *Prog. Org. Coat.* **2005**, *54*, 134
(38) Ellison, C. J.; Ruszkowski, R. L.; Fredin, N. J.; Torkelson1, J. M. *Phys. Rev. Lett.* **2004**, *92* (9), 095702-1.
(39) Kim, J. H.; Jang J.; Zin, W. C. *Langmuir* **2001**, *17*, 2703 and pertinent references therein.
(40) Murayama, T. In *Encyclopedia of Polymer Science and Technology*; Bikales, N. M., Ed.; Wiley-Interscience: New York, 1986; Vol 5, pp 304−309.
(41) Wojciechowska, D. W.; Jeszka, J. K.; Amiens, C.; Chaudret, B.; Lecante, P. *J. Colloid Interface Sci.* **2005**, *287*, 107.
(42) Rault, J. *J. Macromol. Sci., Phys.* **2003**, *B42* (6), 1235−1247.
(43) Asano, A.; Takegoshi, K. *J. Chem. Phys.* **2001**, *115* (18), 8665−8669.
(44) Binder, K. *J. Non-Cryst. Solids* **2002**, *307*−*310*, 1−8.
(45) McLeish, T.; Olmsted, P.; Hamley, I. *R. Soc. Chem. Spec. Publ.* **2001**, *263*, 223−239.
(46) Wellinghoff, S. T.; Baer, E. *J. Appl. Polym. Sci.* **1978**, *22* (7), 1025−2045.
(47) Barbieri, A.; Campani, E.; Capaccioli, S.; Leporini, D. *J. Chem. Phys.* **2004**, *120* (1), 437−453.
(48) Machida, S.; Tanaka, S.; Horie, K. *Polym. Mater. Sci. Eng.* **1997**, *76*, 332−333.
(49) Simpson, J. O.; Bidstrup, S. A. *J. Polym. Sci., Part B: Polym. Phys.* **1993**, *31* (5), 609−18.
(50) Smirnov, V. N. *Kinet. Catal.* **1993**, *34*, 523.
(51) Cataliotti, R.; Foffani, A.; Marchetti, L. *Inorg. Chem.* **1971**, *10* (8), 1594.
(52) Bor, G. *Inorg. Chim. Acta* **1969**, *3* (2), 191−195.
(53) Bor, G. *Spectrochim. Acta* **1962**, *18*, 817−822.
(54) Bigorgne, M. *J. Oragnometal. Chem.* **1970**, *24* (1), 211-229.
(55) Jiang, Y.; Lee, T.; Rose-Petruck, C. G. *J. Phys. Chem. A* **2003**, *107* (38), 7524−7538.
(56) Peden, C. H. F.; Parker, S. F.; Barrett, P. H.; Pearson, R. G. *J. Phys. Chem.* **1983**, *87* (13), 2329−36.
(57) Brown, J. D.; Tevault, D. E.; Cormier, A. D.; Nakamoto, K. *Spectrochim. Acta, Part A* **1975**, *31A* (11), 1773−1774.
(58) Griffith, P. R.; de Haseth, J. A. *Fourier Transform Infrared Spectroscopy*; John Wiley & Sons: New York, 1986.
(59) Roberts, G. E.; White, E. F. T. *The Physics of Glassy Polymers*; Haward, R. N., Ed.; Applied Science Publication: London, 1973.
(60) Livne, S.; Meirovitch, H. *J. Chem. Phys.* **1988**, *88* (7), 4498−4506.
(61) Meirovitch, H. *J. Chem. Phys.* **1988**, *89* (4), 2514−2522.
(62) Raval, R. *J. Phys.: Condens. Matter* **2002**, *14* (16), 4119−4132.
(63) Horie, K.; Mita, I.; *Adv. Polym. Sci.* **1989**, *88*, 77−128.

MA071816O